IEEE Access
Multidisciplinary | Rapid Review | Open Access Journal

Received June 30, 2019, accepted July 16, 2019, date of publication July 26, 2019, date of current version August 9, 2019.

Digital Object Identifier 10.1109/ACCESS.2019.2931324

Application of Fractional Order Sliding Mode Control for Speed Control of Permanent Magnet Synchronous Motor

FARDILA M. ZAIHIDEE[1,2], (Student Member, IEEE), SAAD MEKHILEF[1], (Member, IEEE), AND MARIZAN MUBIN[3], (Member, IEEE)

[1]Power Electronics and Renewable Energy Research Laboratory (PEARL), Department of Electrical Engineering, Faculty of Engineering, University of Malaya, Kuala Lumpur 50603, Malaysia
[2]Faculty of Technical and Vocational, Sultan Idris Education University, Tanjong Malim 35900, Malaysia
[3]Department of Electrical Engineering, Faculty of Engineering, University of Malaya, Kuala Lumpur 50603, Malaysia

Corresponding authors: Saad Mekhilef (saad@um.edu.my) and Fardila M. Zaihidee (farrmz@yahoo.com)

This work was supported in part by the University of Malaya, Malaysia, through the University of Malaya Research Grant Programme (UMRG), under Grant RP043B-17AET, and in part by the Interdisciplinary Research Programme Grant (IIRG), under Grant IIRG011A-2019.

ABSTRACT This paper investigates speed regulation of permanent magnet synchronous motor (PMSM) system based on sliding mode control (SMC). Sliding mode control has been vastly applied for speed control of PMSM. However, continuous SMC enhancement studies are executed to improve the performance of conventional SMC in terms of tracking and disturbance rejection properties as well as to reduce chattering effects. By introducing fractional calculus in the sliding mode manifold, a novel fractional order sliding mode controller is proposed for the speed loop. The proposed fractional order sliding mode speed controller is designed with a sliding surface that consists of both fractional differentiation and integration. Stability of the proposed controller is proved using Lyapunov stability theorem. The simulation and experimental results show the superiorities of the proposed method in terms of faster convergence, better tracking precision and better anti-disturbance rejection properties. In addition, chattering effect of this enhanced SMC is smaller compared to those of conventional SMC. Last but not least, a comprehensive comparison table summarizes key performance indexes of the proposed controller with respect to conventional integer order controller.

INDEX TERMS Fractional calculus, permanent magnet synchronous motor, sliding mode control, speed control.

NOMENCLATURE

DC	Direct current.
DSP	Digital signal processor.
FIR	Finite Impulse Response.
FOSMC	Fractional order sliding mode controller.
FPGA	Field-programmable gate array.
IOSMC	Integer order SMC.
PMSM	Permanent magnet synchronous motors.
SMC	Sliding mode control.
aD_t^r	Fractional calculus fundamental operator.
r	Order of operation of fractional calculus.
$\in$	Element of.
$\mathcal{R}$	Real number.
$\Gamma(.)$	Gamma function.
$PI^{\alpha}D^{\beta}$	Fractional PID.
α	Order of fractional integration.
β	Order of fractional differentiation.
u_d^*, u_q^*	d, q-axis stator voltage.
i_d^*, i_q^*	d, q-axis stator current.
L_d, L_q	d, q-axis stator inductance.
T_e	Electric torque.
I_{df}	Equivalent d-axis magnetizing current.
L_{md}	d-axis mutual inductance.
n_p	Pole pair.
ω_f	Inverter frequency.
ω_r	Rotor speed.
λ_d, λ_q	d, q-axis stator flux linkage.
J	Moment of inertia.
B_m	Viscous friction coefficient.
T_L	Load torque.
k_p, k_i, k_d	Controller coefficients.

The associate editor coordinating the review of this manuscript and approving it for publication was Muhammad Zubair.

$s(t)$ Sliding surface.
$e(t)$ Speed tracking error.
R Stator resistance.

I. INTRODUCTION

Fractional calculus has emerged theoretically since 300 years ago, but only in recent decades has been applied practically in a wide range of science and engineering disciplines. It is a generalization of the traditional integer order integration and differentiation to the non-integer order. Fractional order term has the property of attenuating old data and storing new data, hence is more stable or at least as stable as the integer order counterpart [1], [2]. Fractional calculus theory is applied mainly in four aspects, namely in plant or system models, estimators, optimization algorithms and controllers.

Researchers have grown interest in modeling their systems/plants using fractional calculus to better interpret complex phenomena, processes and system dynamics. Among proposed fractional modeling are electrical components and circuits e.g. inductor [3], supercapacitor [4], [5], memristor [6], fractor [7], [8], oscillator [9], resonator [10] and filter [11], [12] etc., hydraulic turbine governing system [13], magnetorheological vibration device [14] and FIR differentiator [15]. Advantages of fractional order modeling against integer order modeling include improves reliability due to consideration of non-ideal properties [16], reduces computational complexity when combined with fractional controllers [17], electronic tuning capability [10] and has better accuracy [14] as well as real-time performance [5]. Apart from being applied in plant or system modeling, this non-integer calculus theory is also used for various kinds of estimator design in a vast area of application e.g. fractional order compensators [18], [19], fractional order observer [20] and fractional order sliding mode observer [21]. Inherent strengths of fractional calculus in terms of long-term memory, nonlocality and weak singularity makes it preferable to be applied in optimization problems such as signal and image processing [22], [23] and complex neural network training [24].

Last but not least, fractional calculus has also been incorporated in controllers design. Extensively, the theory is integrated with classical PID control theory to come out with fractional PID controllers indicated as $PI^{\lambda}D^{\mu}$ [25]–[27], which recent development, design and tuning methods are thoroughly reviewed in [28]. Superiorities of $PI^{\lambda}D^{\mu}$ controllers have drawn researchers to consider fractional calculus to enhance their controllers. Other fractional order controllers emerged which includes fractional adaptive controllers [29], [30] and fractional order sliding mode control [21], [31]–[33]. State-of-the-art fractional controls and their enormous advantages have been reviewed in details for various kinds of systems such as for time delay systems [34], for unmanned vehicles [35] and for industrial automation [36].

FOSMC utilizes fractional calculus in constructing its sliding surface. The extra degree of freedom of integral and derivative operators can improve the controller's performance further compared to traditional IOSMC. FOSMC has proven its advantages against IOSMC in many areas of application e.g. smaller total harmonic distortion, eliminates system uncertainties and reduces tracking error in active power filter [37], [38], faster deployment without overshoot and less chattering in deployment of space tethered system [39] and faster response, smaller tracking error, disturbance and noise signals rejection capability and robustness against uncertainty in nuclear reactors [40].

This paper aims to further investigate the advantage of incorporating fractional calculus in SMC for controlling real systems e.g. electrical machines. Implementation of fractional controllers on electrical machines such as DC motors, induction generators and permanent magnet linear synchronous motors have resulted in better transient response, better convergence properties and lower chattering than other controllers in comparison [41]–[43]. Permanent magnet synchronous motors are widely used in low to mid power application and high performance drives e.g. robotics, electric vehicles and machine tools. They are preferred over brush-type motors and gradually replacing induction motors in various fields of application due to its advantages such as compact structure, high air-gap flux density, high power density, high torque to inertia ratio, and high efficiency. However, PMSM system is nonlinear and consists of time-varying parameters with high-order complex dynamics [44], [45]. High performance application of PMSM requires its speed controller to result in fast response, precise tracking, small overshoot and strong disturbance rejection ability. Linear control algorithms e.g. PI controllers have been widely used for speed control of PMSM, but the performances were unsatisfactory in terms of tracking ability and robustness [46]. Hence, robust nonlinear control methods have been proposed and used to enhance speed control performance of PMSM. These methods include sliding mode control [2], [44]–[48], predictive control [49], [50], backstepping control [51], adaptive control [52]–[54], H∞ control [55], automatic disturbance rejection control [56] and artificial intelligence incorporated controllers [57], [58].

Sliding mode control has been vastly applied for speed control of PMSM. Various SMC enhancement methods have been proposed to improve the performance of conventional SMC in terms of tracking and disturbance rejection properties as well as to reduce chattering effects. These methods include sliding surface design modification, reaching law methods, higher order SMC and composite SMC designs e.g. combination with artificial intelligence or disturbance compensation, as summarized in Fig. 1. A thorough review of enhancement methods in SMC for PMSM control is reviewed in [59].

In this paper, conventional SMC is enhanced by modifying its sliding manifold design to obtain a fractional order SMC to control the speed of a PMSM. The proposed FOSMC is designed with differentiation and integration sliding surface.

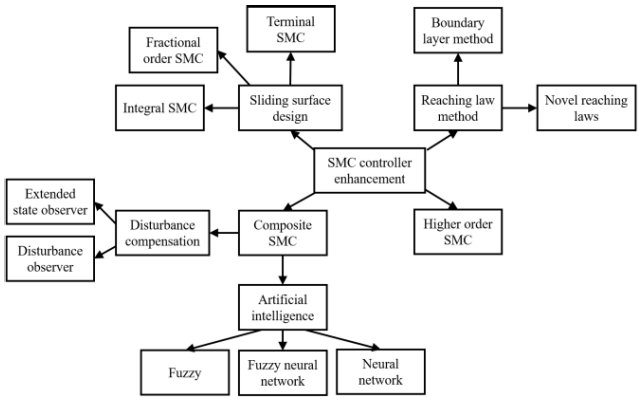

FIGURE 1. Summary of SMC enhancement methods [59].

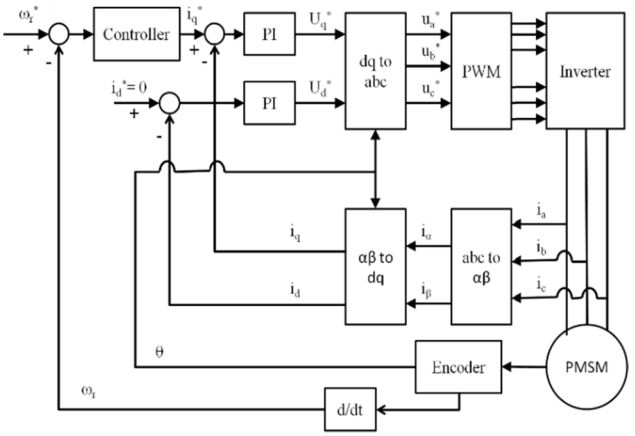

FIGURE 2. Field-oriented speed control of PMSM.

The effectiveness of the proposed controller for PMSM is verified using simulation and experimental approach. Its performance is compared against conventional SMC to prove its superiority.

The rest of the paper is organized in the following manner. Fractional calculus is briefly introduced and defined in Section II. The proposed fractional order SMC design is described in Section III. Simulation and experimental results are presented and analyzed in Section IV. Finally, conclusions and future works are given in Section V.

II. FRACTIONAL CALCULUS THEORY AND DEFINITION

Fundamental operator of fractional calculus ${}_aD_t^r$ is defined as in (1), where a and t are the limits of the operation and r is the order of operation. r is generally $r \in R$ but r could also be a complex number [60].

$$ {}_aD_t^r = \begin{cases} \dfrac{d^r}{dt^r} & forr > 0, \\ 1 & forr = 0, \\ \int_a^t (d\tau)^{-r} & forr < 0, \end{cases} \tag{1} $$

Three definitions are commonly used for the general fractional differintegral namely the Grunwald-Letnikov definition (2), the Riemann-Liouville definition (3) and the Caputo definition (4) for $n-1 < r < n$. Riemann-Liouville definition of fractional differintegral is also formulated in form of Laplace transformation (5) for $n-1 < r \leq n$ and $s \equiv j\omega$ which denotes the Laplace transform variable, since this method is commonly used in engineering problem solving [61], [62].

$$ {}_aD_t^r f(t) = \lim_{h\to 0} h^{-r} \sum_{j=0}^{\left[\frac{t-a}{h}\right]} (-1)^j \binom{r}{j} f(t-jh) \tag{2} $$

$$ {}_aD_t^r f(t) = \frac{1}{\Gamma(n-r)} \frac{d^n}{dt^n} \int_a^t \frac{f(\tau)}{(t-\tau)^{r-n1}} d\tau \tag{3} $$

$$ {}_aD_t^r f(t) = \frac{1}{\Gamma(r-n)} \int_a^t \frac{f^{(n)}(\tau)}{(t-\tau)^{r-n1}} d\tau \tag{4} $$

$$ \int_0^\infty e^{-st} {}_0D_t^r f(t)dt = s^r F(s) - \sum_{k=0}^{n-1} s^k {}_0D_t^{r-k-1} f(t)\,|t=0 \tag{5} $$

Understanding of geometric and physical of fractional differentiation and integration compared to integer order ones is detailed in Podlubny [63]. Furthermore, main properties of fractional calculus are listed in Chen *et al.* [60].

III. DESIGN OF FRACTIONAL ORDER SMC FOR PMSM SPEED CONTROL

A. CONTROLLER DESIGN

In the proposed controller, field-oriented control of PMSM as illustrated in Fig. 2 is chosen, which mathematical model is described as in (6)-(8). d, q-axis stator flux linkages are defined in (9) and (10) and motor dynamics is described in (11).

$$ u_d^* = R_s i_d^* + \dot{\lambda}_d - \omega_f \lambda_q \tag{6} $$

$$ u_q^* = R_s i_q^* + \dot{\lambda}_q + \omega_f \lambda_d \tag{7} $$

$$ T_e = 1.5 n_p \left[L_{md} I_{df} i_q^* + \left(L_d - L_q\right) i_d^* i_q^* \right] \tag{8} $$

$$ \lambda_q = L_q i_q^* \tag{9} $$

$$ \lambda_d = L_d i_d^* + L_{md} I_{df} \tag{10} $$

$$ T_e = J\dot{\omega}_r + B_m \omega_r + T_L \tag{11} $$

In this study, the main control problem is to ensure the motor speed, ω_r to track the desired speed command, ω_r^* asymptotically. The speed tracking error, e(t) is defined in (12). The main speed controller i.e., the sliding mode controller provides an output in terms of q-axis stator current command, i_q as the control input for the inner q-axis current controller.

$$ e(t) = \omega_r^*(t) - \omega_r(t) \tag{12} $$

The proposed fractional PID ($PI^\alpha D^\beta$) sliding surface is defined in (13), where ${}_0D_t^{-\alpha}$ (.) is a fractional integration of order α and ${}_0D_t^{\beta}$ (.) is a fractional differentiation of order β.

By selecting $\alpha = \beta = 1$, a classical integer order PID sliding surface is obtained. With the chosen control law (14), the equivalent control law (15) is obtained.

$$s(t) = k_p e(t) + k_{i0} D_t^{-\alpha} e(t) + k_{d0} D_t^{\beta} e(t)$$
$$k_p, k_i, k_d > 0, \quad 0 < \alpha < 1, \quad 0 < \beta < 1 \tag{13}$$
$$\dot{s} = -ws - k_s \text{sign}(s), w, k_s \in R^+ \tag{14}$$
$$i_q^*(t) = \left(bk_p\right)^{-1} \begin{bmatrix} k_{i0} D_t^{1-\alpha} e(t) + k_{d0} D_t^{\beta+1} e(t) \\ +(w-a) k_p e(t) \\ +k_p \emptyset(t) + w k_{i0} D_t^{-\alpha} e(t) \\ +w k_{d0} D_t^{\beta} e(t) + k_s sign(s) \end{bmatrix} \tag{15}$$

B. STABILITY ANALYSIS

Reaching condition of the proposed fractional sliding manifold has to be satisfied to ensure convergence of system state to the manifold for any initial condition. For this purpose, Lyapunov stability theorem is used, where the Lyapunov function candidate is chosen to be $V = (1/2)s^2$ for system initial states $t_0 \neq 0$. The reaching condition is satisfied when $\dot{V} < 0$ holds or $s\dot{s} < 0$. From (16), it shows that $\dot{V} < 0$ holds when $k_s > k_p |\delta(t)|$ is satisfied or $(k_s/k_p) > |\delta(t)|$ is satisfied. Assumed that $|\delta(t)| \leq \emptyset \in R^+$, then, according to Lyapunov stability theorem, the reaching condition of the proposed FOSMC is satisfied if $(k_s/k_p) > \emptyset$. In addition, Zhang *et al.* [2] has proven that with the chosen control law, system will converge to the switching manifold at any initial state when inequality (17) is satisfied.

$$\dot{V} = -ws^2 - k_s |s| + k_p \delta(t) s \tag{16}$$
$$t \geq t_0 - (1/w) ln(k_s/w |s(t_0)| + k_s) \tag{17}$$

After reaching condition is ensured, the stability of the system during sliding phase has to be analyzed. For that purpose, Lemma below is presented, followed by its corresponding theorem and proof.

Lemma: [64] The following autonomous fractional order system is considered,

$${}_0D_t^r x(t) = A.x(t), x(0) = x_0 \tag{18}$$

where $x \in R^n, A = \left(a_{ij}\right) \in R^{nxn}, 0 < r < 1$, is asymptotically stable if and only if

$$|arg(eig(A))| > r(\pi/2) \tag{19}$$

Theorem: System in (13) is stable when conditions $k_p, k_I, k_d > 0$ and $0 < \alpha, \beta < 1$ are synchronously satisfied.

Proof. When sliding mode occurs, the sliding mode dynamics are represented in matrix form as in (20).

$$\begin{bmatrix} {}_0D_t^{\alpha}(e_1) \\ {}_0D_t^{\beta}(e_2) \end{bmatrix} = \begin{bmatrix} 0 & 1 \\ -(k_i/k_d) & -(k_p/k_d) \end{bmatrix}$$
$$\begin{bmatrix} e_1 \\ e_2 \end{bmatrix} = A \begin{bmatrix} e_1 \\ e_2 \end{bmatrix} \tag{20}$$

By Lemma, system (13) is stable if the condition in (19) is satisfied. Since $0 < \alpha, \beta < 1$ is satisfied, hence, $0 < \alpha(\pi/2) < (\pi/2)$ and $0 < \beta((\pi/2) < (\pi/2)$. Stability condition in Lemma is satisfied if k_p, k_i and k_d are selected to be positive.

TABLE 1. Parameters of PMSM.

Parameter	Value
Stator resistance, R_s	1.2 Ω
d-axis stator inductance, L_d	6.35 m H
q-axis stator inductance, L_q	6.75 m H
Moment of inertia, J	2.31×10^{-4} kg m^2
Viscous friction coefficient, B_m	0.0002 Nm s
Flux linkage, λ_f	0.15 Wb
Pole pair, n_p	4

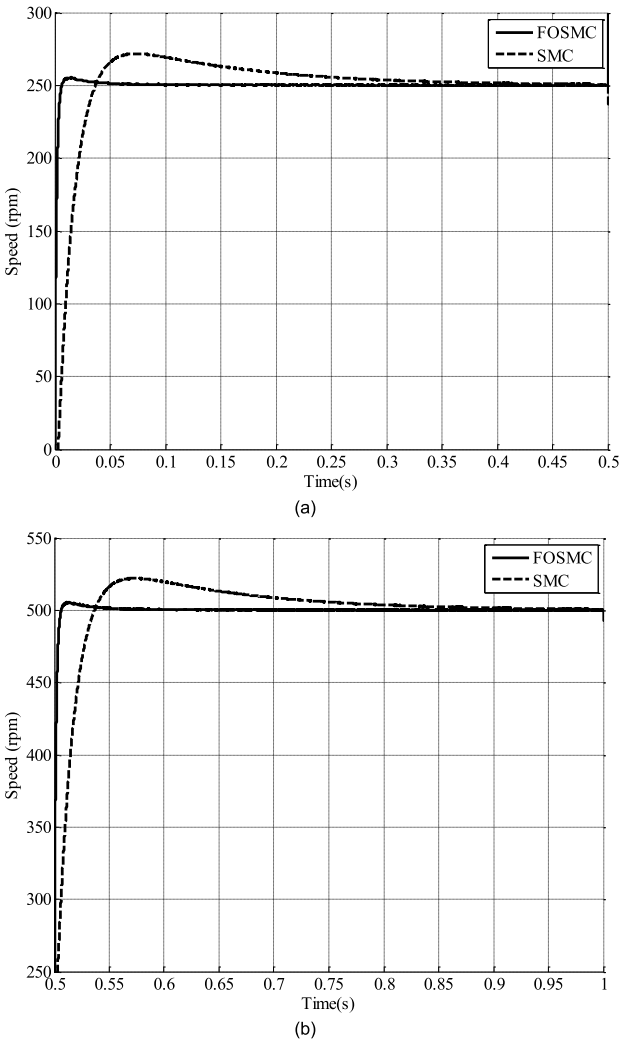

FIGURE 3. Speed response comparison between FOSMC and SMC for speed reference of (a) 250 rpm (b) 500 rpm (simulation).

IV. RESULTS AND DISCUSSION

A. SIMULATION RESULTS

Performance of the proposed controller is evaluated using simulation in MATLAB/Simulink environment. The PMSM model used in this simulation is a three-phase Y-connected 1.93 kW motor with parameters as listed in Table 1. Fractional orders α and β of the designed controller was chosen to be 0.35 and 0.3 respectively.

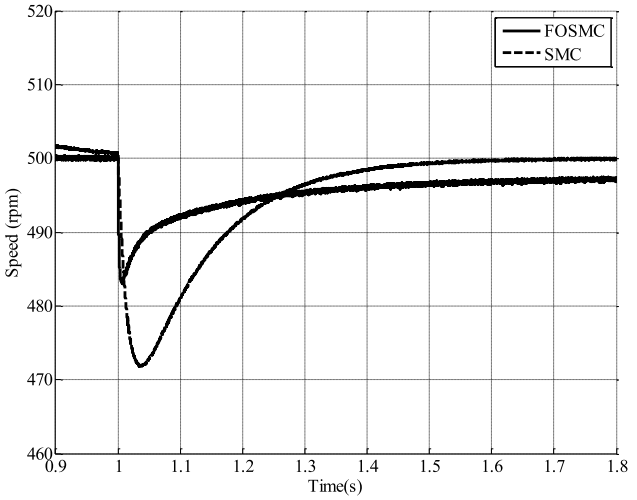

FIGURE 4. Comparison of speed drop of FOSMC and SMC under 0.5 Nm load (simulation).

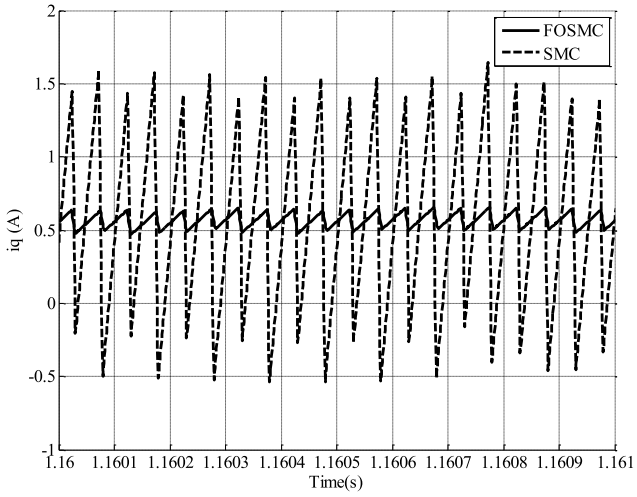

FIGURE 5. Comparison of q-axis reference current as output of FOSMC and SMC speed controllers (simulation).

In simulation evaluation, a speed reference of 250 rpm was given for 0.5 seconds, followed by 500 rpm speed reference for another 0.5 seconds. The step response for both scenarios is shown in Fig. 3(a) and Fig. 3(b) respectively. Similar results were obtained in both cases where FOSMC-controlled system produced less overshoot and tracked the reference faster compared to SMC system.

Disturbance rejection properties of the proposed controller were evaluated by giving a load of 0.5 Nm at t = 1s. Results in Fig. 4 shows that system driven with FOSMC suffered approximately half speed drop compared to SMC and settled with a small steady state error of only 0.6%. When load is applied, q-axis reference current i.e. speed controller output of both controllers in comparison is as shown in Fig. 5. FOSMC speed controller produces reference value with almost 20 times less ripple. In addition, as shown in Fig. 6, system with FOSMC resulted in less torque ripple compared to system driven with SMC.

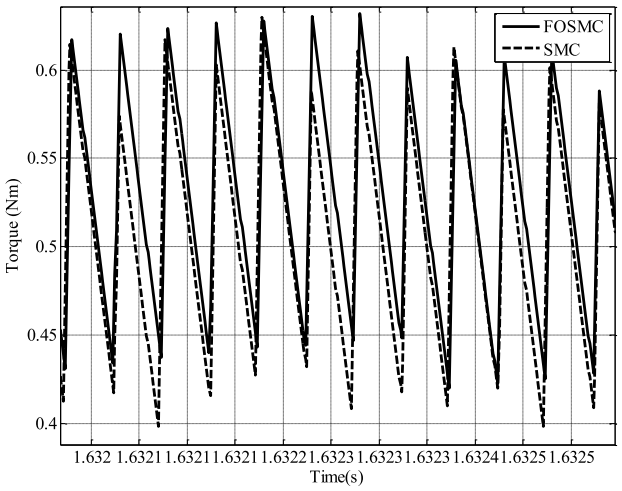

FIGURE 6. Torque ripple comparison between FOSMC and SMC (simulation).

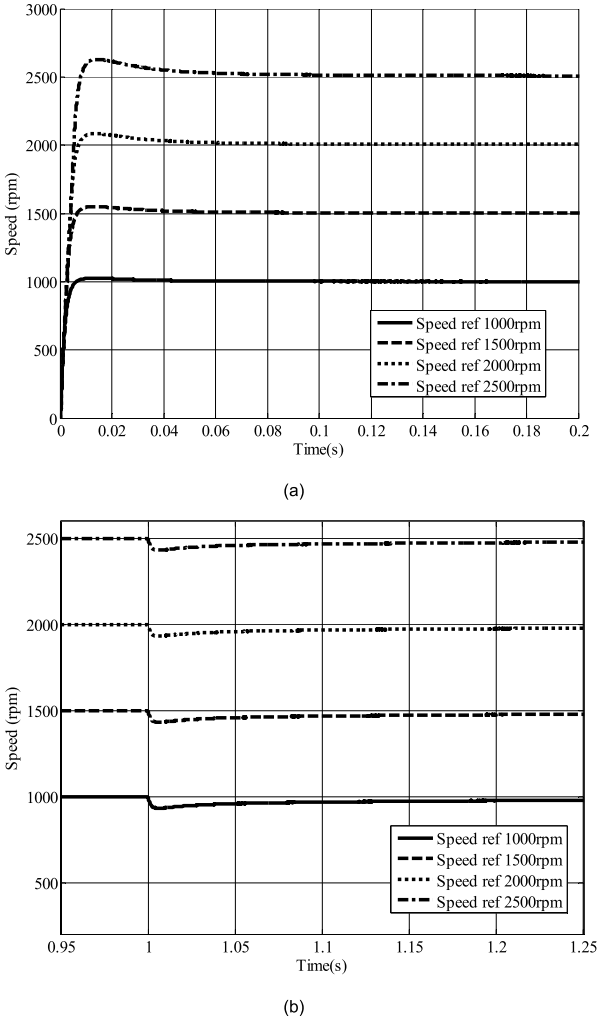

FIGURE 7. Speed response of FOSMC for various speed reference (a) at no load (b) when load of 2 Nm is applied (simulation).

Performance of the proposed FOSMC is further validated for various speed references between 1000 to 2500 rpm

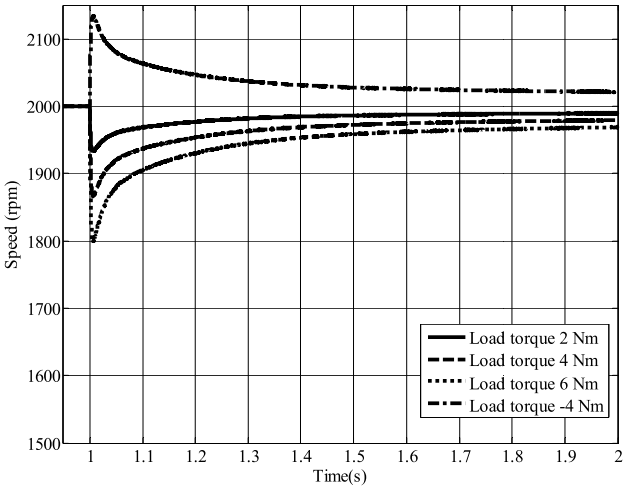

FIGURE 8. Speed drop of FOSMC under various loads (simulation).

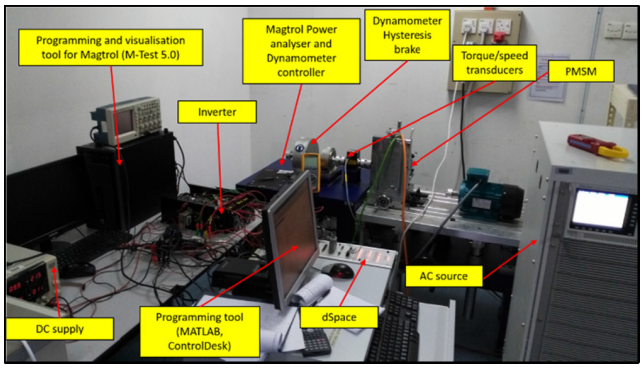

FIGURE 9. PMSM system prototype.

with load torque of 2 Nm applied after 1 second. Results in Fig. 7(a) shows that given reference speeds were successfully tracked with maximum overshoot of only 5.04% namely for speed reference of 2500 rpm. When load torque is applied, the system suffered from speed drop of only between 2.28% and 6.06%, before settled back to its reference speed after approximately 0.25 seconds, as shown in Fig. 7(b). Fig. 8 shows speed drop of FOSMC driven PMSM system with reference speed of 2000 rpm when various loads are applied. In all cases, speed recovers back to reference speed after not more than 9.8% speed drop with maximum steady state error of only 1.1% (at load 6 Nm).

B. EXPERIMENTAL RESULTS

In addition to simulation, the robustness and stability of the proposed control scheme are verified through actual experiment. The prototype of PMSM speed control, as shown in Fig. 9 consists of a PMSM with built-in encoder (parameters in Table 1), driven by a three-phase voltage source PWM inverter. DSpace DS1104 performs as the controller, which signals can be monitored using the ControlDesk software. Required load is given by Magtrol hysteresis brake AHB-3. The brake is controlled by Magtrol DSP6001 controller, which can be programmed using Magtrol M-TEST

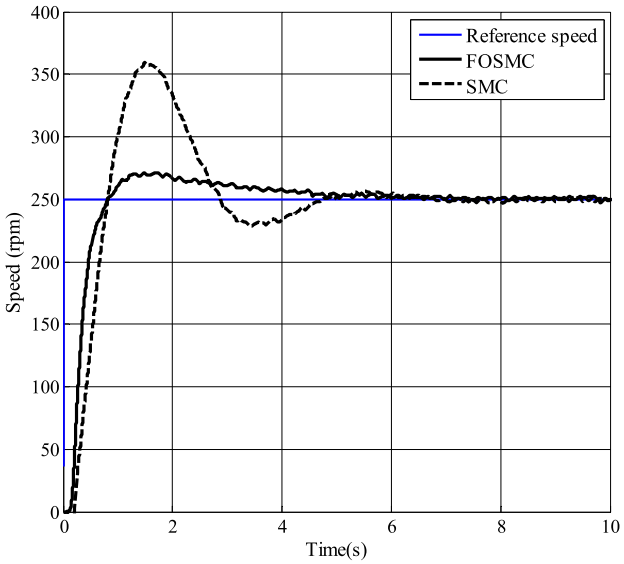

FIGURE 10. Speed response comparison between FOSMC and SMC for speed reference of 250 rpm (experimental).

5.0 Motor Testing software. TMB 307/411 in-line torque and speed transducer provides torque and speed measurement. Auxiliary components such as current sensors and encoder data interface circuits are also designed and built into the prototype.

In experimental verification, PMSM system prototype was tested with the proposed fractional order SMC controller as well as with a conventional integer order SMC for comparison purpose. Firstly, a speed reference of 250 rpm was given to investigate the step speed response of both cases. Fig. 10 compares the speed response of PMSM for speed reference of 250 rpm when controlled with a FOSMC and a conventional SMC. System using FOSMC resulted in only 8.32% overshoot, which is about 5 times smaller than the overshoot obtained when using SMC. Some speed oscillation was experienced by SMC-controlled system as response to the step change. Speed ripple of both cases at steady state were also investigated where FOSMC recorded 1.56% maximum ripple compared to 1.36% of SMC, as shown in Fig. 11.

Then, from 250 rpm, the speed reference was doubled to 500 rpm to evaluate controller's performance at a different speed. As shown in Fig. 12, the results obtained are similar to the previous case. The fosmc-controlled system recorded 5 times smaller overshoot than those of SMC-controlled system and did not suffer under step change oscillation.

Disturbance rejection properties of the proposed controller and the controller in comparison were investigated by giving a load of approximately 0.5 Nm to the system after about 10 seconds. From speed 500 rpm, the prototype suffered a speed drop of 27.4 rpm under the given load when controlled with the proposed fractional order controller. 35% more speed drop was experienced by the prototype when controlled by SMC. During speed recovery, it can be seen in Fig. 13 that

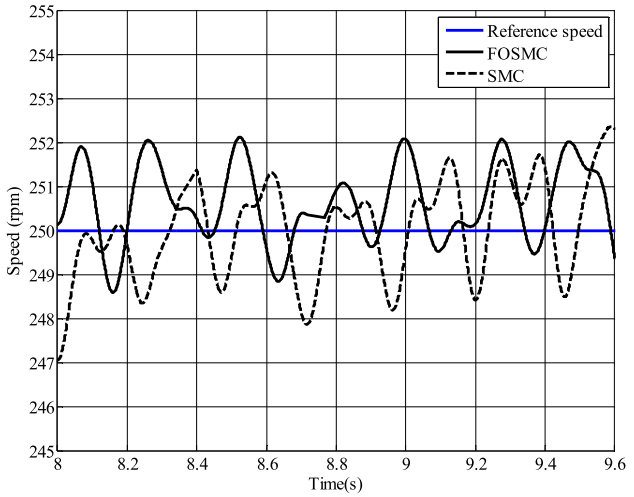

FIGURE 11. Speed ripple of FOSMC and SMC during steady state (experimental).

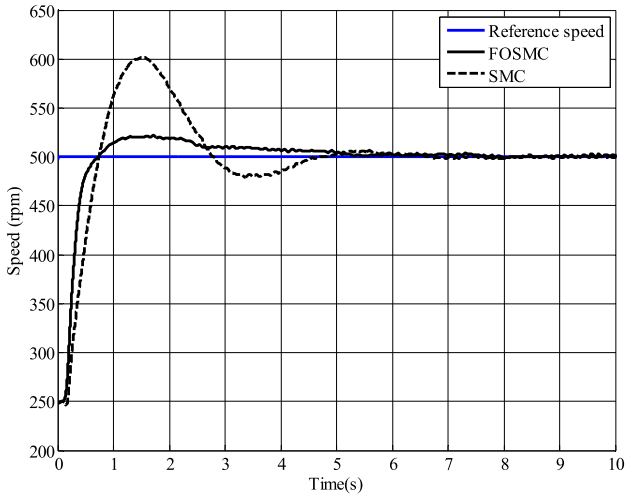

FIGURE 12. Speed response comparison between FOSMC and SMC for speed reference of 500 rpm (experimental).

FOSMC-system settled after about 6 seconds to the speed reference with a small steady-state error of only 0.46%. On the other hand, SMC-system oscillates at early stage of recovery with 3.32% of overshoot before settling back to the speed reference and continue to oscillate at 0.5%.

Fig. 14 shows changes in q-axis reference current when load was given and the corresponding actual q-axis current in the FOSMC and SMC systems. Current, i_q ripple in both cases can be compared from Fig. 14(a) and 14(b), where i_q ripple in FOSMC is less than those in SMC of approximately 6%. Speed controller output i.e. the reference q-axis current produced by both controllers are compared Fig. 15. The proposed controller required about 20% less current spike at load increase and settled with less oscillation compared to the SMC controller in comparison. In addition to that, when controlled with FOSMC, the motor experienced less torque ripple compared to when controlled with SMC as shown in Fig. 16.

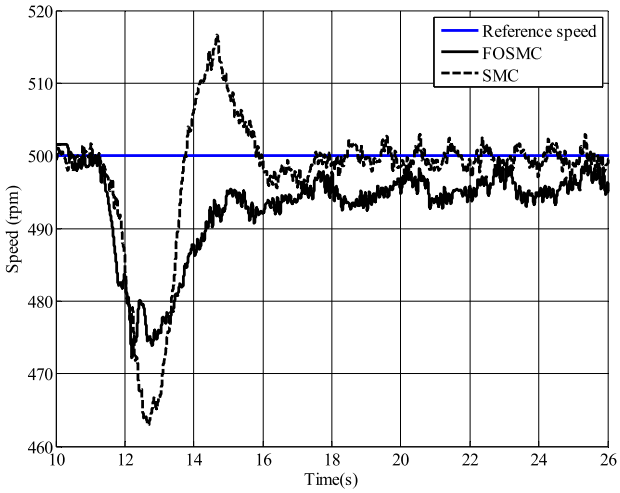

FIGURE 13. Speed drop of FOSMC and SMC under 0.5 Nm load (experimental).

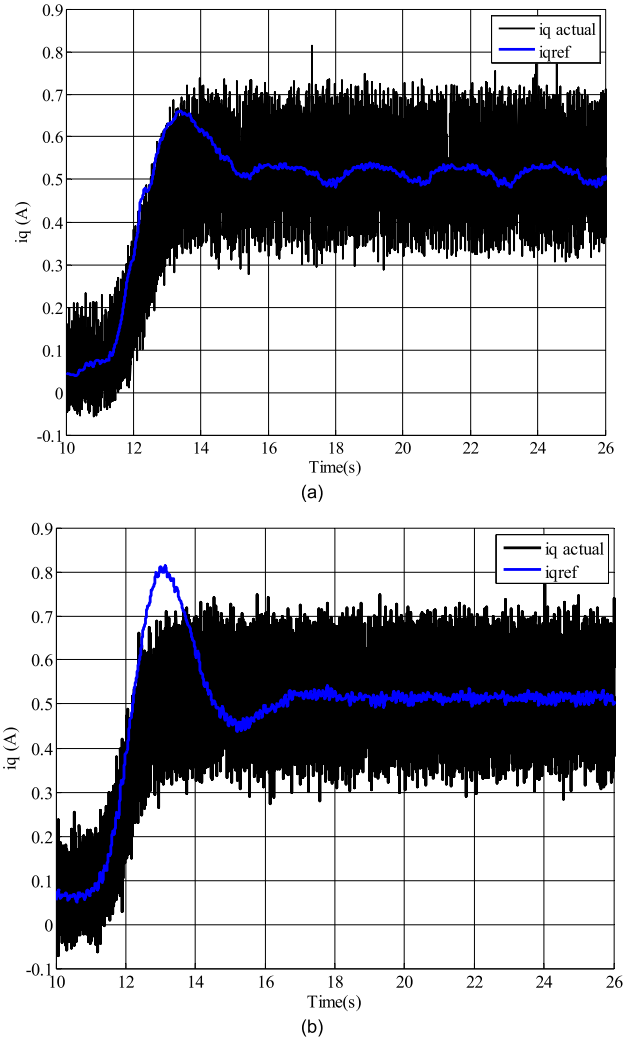

FIGURE 14. Reference and actual q-axis current under 0.5 Nm load for (a) FOSMC system (b) SMC system (experimental).

Lastly, the controllers were further tested by removing the given load from the system at around t = 27s. Fig. 17 shows

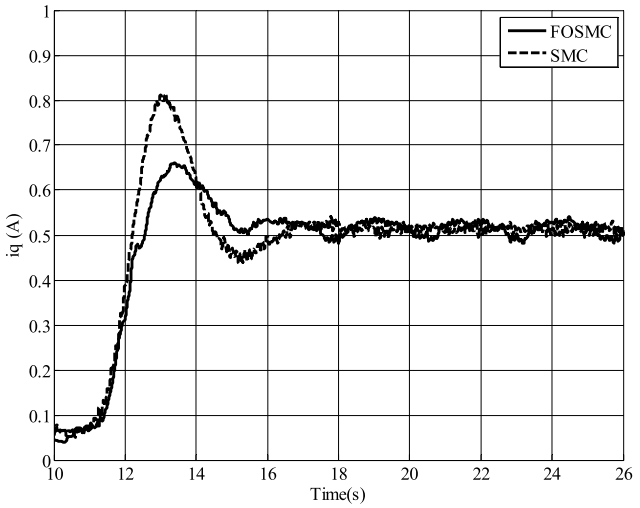

FIGURE 15. Comparison of q-axis reference current as output of FOSMC and SMC speed controllers (experimental).

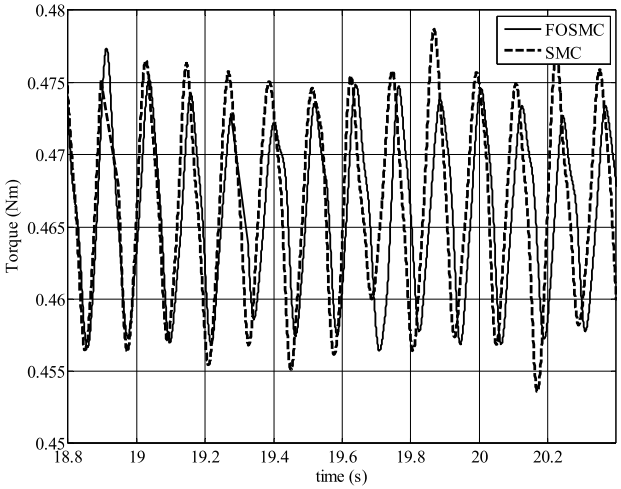

FIGURE 16. Torque ripple comparison between FOSMC and SMC (experimental).

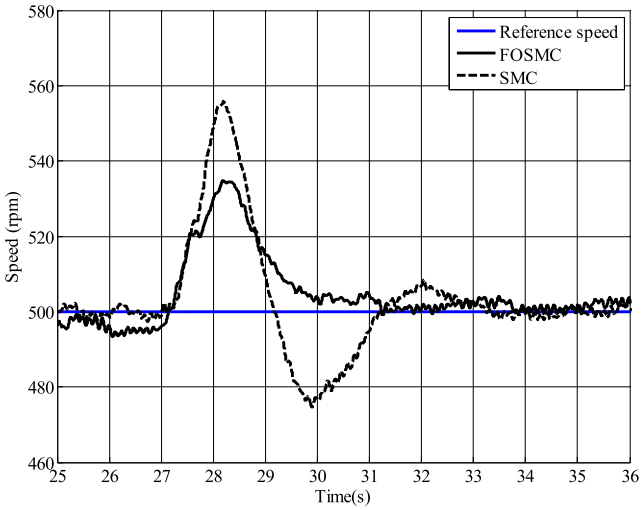

FIGURE 17. Speed response of FOSMC and SMC when load was removed.

TABLE 2. Summary of simulation and experimental results.

Properties	FOSMC (proposed)	SMC (conventional)
Simulation results (Speed reference = 500 rpm, Load torque = 0.5 Nm)		
Overshoot (%)	1.06	4.4
Steady state error (%) (no load)	0	0
Speed drop (%)	3.32	5.62
Steady state error (%) (with load)	0.6	0
Recovery time (s)	1.5	1.5
Torque ripple (Nm)	0.1834	0.2188
Experimental results (Speed reference = 500 rpm, Load torque = 0.5 Nm)		
Rise time (s)	0.73	0.74
Overshoot (%)	4.14	20.38
Steady state error (%) (no load)	0	0
Speed drop (%)	5.48	7.4
Steady state error (%) (with load)	0.46	0
Recovery time (s)	6	6
Torque ripple (Nm)	0.0172	0.0194

that with only 6.92% speed increase, speed of motor in FOSMC system settled back to 500 rpm after about 4 seconds. In SMC system, the motor experienced a speed hike up to 11.16% and significant oscillation before settling back to the reference speed after about 6 seconds.

It is also important to mention that authors are aware that these experimental results are not totally at par with other data presented in previous literatures especially in terms of rise time and settling time. The experimental validation of the proposed controller is limited by available equipment in our laboratory for building the prototype. Usage of dSpace DS1104 as controller in this prototype limited the sampling time at $5e^{-4}$ s and switching frequency at 4kHz. Higher sampling time and switching frequency can be used by improving the controller to more advanced controllers such as Speedgoat, advanced DSPs or FPGAs. However, authors believe that within this limited capacity, necessary results to show superiorities of the proposed controller and the conventional controller have been presented above.

Summary of both simulation and experimental results are tabulated in Table 2, showing how incorporating fractional calculus affects and improves the performance of a conventional sliding mode speed controller.

V. CONCLUSION AND FUTURE WORKS

A fractional order sliding mode speed controller for PMSM has been proposed in this research. Fractional calculus is incorporated into the sliding surface design. Simulation and

experimental results proved that the proposed FOSMC controller performs better in terms of speed tracking and anti-disturbance properties compared to a conventional SMC controller. The proposed controller also reduces the chattering effect of sliding mode control.

As future works, the proposed controller can be further enhanced by incorporating artificial intelligence tuning mechanism to optimize the controller's parameters to improve its performance. Furthermore, fractional order values used in the controller can be designed to be adaptive depending on the machine dynamics and external disturbances. Other than that, the proposed controller can also be expanded with appropriate estimators to realize sensorless control of electrical machines.

ACKNOWLEDGMENT

The authors would like to thank Dr. Che Hang Seng from UM Power Energy Dedicated Advanced Centre (UMPEDAC) for assistance in realizing the experimental setup used in this work.

REFERENCES

[1] J. Huang, L. Cui, X. Shi, H. Li, and Z. Xiang, "Composite integral sliding mode control for PMSM," in *Proc. CCC*, Nanjing, China, Jul. 2014, pp. 8086–8090.

[2] B. Zhang, Y. Pi, and Y. Luo, "Fractional order sliding-mode control based on parameters auto-tuning for velocity control of permanent magnet synchronous motor," *ISA Trans.*, vol. 51, pp. 649–656, Sep. 2012.

[3] A. Soltan, A. G. Radwan, and A. M. Soliman, "Fractional-order mutual inductance: Analysis and design," *Int. J. Circuit Theory Appl.*, vol. 44, no. 1, pp. 85–97, Jan. 2016.

[4] R. Kopka, "Changes in derivative orders for fractional models of supercapacitors as a function of operating temperature," *IEEE Access*, vol. 7, pp. 47674–47681, 2019.

[5] J. Wang, L. Zhang, J. Mao, J. Zhou, and D. Xu, "Fractional order equivalent circuit model and SoC estimation of supercapacitors for use in HESS," *IEEE Access*, vol. 7, pp. 52565–52572, 2019.

[6] Y. Pu and X. Yuan, "Fracmemristor: Fractional-order memristor," *IEEE Access*, vol. 4, pp. 1872–1888, 2016.

[7] Y.-F. Pu, "Measurement units and physical dimensions of fractance—Part I: Position of purely ideal fractor in Chua's axiomatic circuit element system and fractional-order reactance of fractor in its natural implementation," *IEEE Access*, vol. 4, pp. 3379–3397, 2016.

[8] Y.-F. Pu, "Measurement units and physical dimensions of fractance—Part II: Fractional-order measurement units and physical dimensions of fractance and rules for fractors in series and parallel," *IEEE Access*, vol. 4, pp. 3398–3416, 2016.

[9] A. G. Radwan, A. S. Elwakil, and A. M. Soliman, "Fractional-order sinusoidal oscillators: Design procedure and practical examples," *IEEE Trans. Circuits Syst. I, Reg. Papers*, vol. 55, no. 7, pp. 2051–2063, Aug. 2008.

[10] G. Tsirimokou, C. Psychalinos, A. S. Elwakil, and K. N. Salama, "Electronically tunable fully integrated fractional-order resonator," *IEEE Trans. Circuits Syst. II, Exp. Briefs*, vol. 65, no. 2, pp. 166–170, Feb. 2018.

[11] A. S. Ali, A. G. Radwan, and A. M. Soliman, "Fractional order Butterworth filter: Active and passive realizations," *IEEE J. Emerg. Sel. Topics Circuits Syst.*, vol. 3, no. 3, pp. 346–354, Sep. 2013.

[12] A. Adhikary, S. Sen, and K. Biswas, "Practical realization of tunable fractional order parallel resonator and fractional order filters," *IEEE Trans. Circuits Syst. I, Reg. Papers*, vol. 63, no. 8, pp. 1142–1151, Aug. 2016.

[13] L. Liu, B. Wang, S. Wang, Y. Chen, T. Hayat, and F. E. Alsaadi, "Finite-time H-infinity control of a fractional-order hydraulic turbine governing system," *IEEE Access*, vol. 6, pp. 57507–57517, 2018.

[14] B. Chen, C. Li, B. Wilson, and Y. Huang, "Fractional modeling and analysis of coupled MR damping system," *IEEE/CAA J. Automatica Sinica*, vol. 3, no. 3, pp. 288–294, Jul. 2016.

[15] C.-C. Tseng, "Design of fractional order digital FIR differentiators," *IEEE Signal Process. Lett.*, vol. 8, no. 3, pp. 77–79, Mar. 2001.

[16] A. Allagui, T. J. Freeborn, A. S. Elwakil, M. E. Fouda, B. J. Maundy, A. G. Radwan, Z. Said, and M. A. Abdelkareem, "Review of fractional-order electrical characterization of supercapacitors," *J. Power Sources*, vol. 400, pp. 457–467, Oct. 2018.

[17] N. Ullah, A. Ullah, A. Ibeas, and J. Herrera, "Improving the hardware complexity by exploiting the reduced dynamics-based fractional order systems," *IEEE Access*, vol. 5, pp. 7714–7723, 2017.

[18] M. S. Tavazoei and M. Tavakoli-Kakhki, "Compensation by fractional-order phase-lead/lag compensators," *IET Control Theory Appl.*, vol. 8, no. 5, pp. 319–329, Mar. 2014.

[19] Y. Luo, Y. Q. Chen, H.-S. Ahn, and Y. G. Pi, "Fractional order periodic adaptive learning compensation for state-dependent periodic disturbance," *IEEE Trans. Control Syst. Technol.*, vol. 20, no. 2, pp. 465–472, Mar. 2012.

[20] I. N. Doye, K. N. Salama, and T. Laleg-Kirati, "Robust fractional-order proportional-integral observer for synchronization of chaotic fractional-order systems," *IEEE/CAA J. Autom. Sinica*, vol. 6, no. 1, pp. 268–277, Jan. 2019.

[21] A. Mujumdar, B. Tamhane, and S. Kurode, "Observer-based sliding mode control for a class of noncommensurate fractional-order systems," *IEEE/ASME Trans. Mechatronics*, vol. 20, no. 5, pp. 2504–2512, Oct. 2015.

[22] H. Singh, A. Kumar, L. K. Balyan, and H.-N. Lee, "Fractional-order integration based fusion model for piecewise gamma correction along with textural improvement for satellite images," *IEEE Access*, vol. 7, pp. 37192–37210, 2019.

[23] A. Kumar, M. O. Ahmad, and M. N. S. Swamy, "A framework for image denoising using first and second order fractional overlapping group sparsity (HF-OLGS) regularizer," *IEEE Access*, vol. 7, pp. 26200–26217, 2019.

[24] J. Wang, G. Yang, B. Zhang, Z. Sun, Y. Liu, and J. Wang, "Convergence analysis of caputo-type fractional order complex-valued neural networks," *IEEE Access*, vol. 5, pp. 14560–14571, 2017.

[25] P. Lanusse, A. Oustaloup, and J. Sabatier, "Robust factional order PID controllers: The first generation CRONE CSD approach," in *Proc. ICFDA*, Catania, Italy, Jun. 2014, pp. 1–6.

[26] B. T. Zhang and Y. Pi, "Robust fractional order proportion-plus-differential controller based on fuzzy inference for permanent magnet synchronous motor," *IET Control Theory Appl.*, vol. 6, no. 6, pp. 829–837, Apr. 2012.

[27] J. Viola, L. Angel, and J. M. Sebastian, "Design and robust performance evaluation of a fractional order PID controller applied to a DC motor," *IEEE/CAA J. Autom. Sinica*, vol. 4, no. 2, pp. 304–314, Apr. 2017.

[28] P. Shah and S. Agashe, "Review of fractional PID controller," *Mechatronics*, vol. 38, pp. 29–41, Sep. 2016.

[29] M. Ö. Efe, "Fractional fuzzy adaptive sliding-mode control of a 2-DOF direct-drive robot arm," *IEEE Trans. Syst., Man, Cybern., B Cybern.*, vol. 38, no. 6, pp. 1561–1570, Dec. 2008.

[30] S. Ladaci and A. Charef, "On fractional adaptive control," *Nonlinear Dyn.*, vol. 43, pp. 365–378, Mar. 2006.

[31] A. J. Calderón, B. M. Vinagre, and V. Feliu, "Fractional order control strategies for power electronic buck converters," *Signal Process.*, vol. 86, pp. 2803–2819, Oct. 2006.

[32] H. Delavari, R. Ghaderi, A. Ranjbar, and S. Momani, "Fuzzy fractional order sliding mode controller for nonlinear systems," *Commun. Nonlinear Sci. Numer. Simul.*, vol. 15, no. 4, pp. 963–978, 2010.

[33] D. Abdelhamid, T. Bouden, and A. Boulkroune, "Design of fractional-order sliding mode controller (FSMC) for a class of fractional-order nonlinear commensurate systems using a particle swarm optimization (PSO) algorithm," *J. Control Eng. Appl. Inform.*, vol. 16, no. 3, pp. 46–55, 2014.

[34] I. Birs, C. Muresan, I. Nascu, and C. Ionescu, "A survey of recent advances in fractional order control for time delay systems," *IEEE Access*, vol. 7, pp. 30951–30965, 2019.

[35] R. Cajo, T. T. Mac, D. Plaza, C. Copot, R. De Keyser, and C. Ionescu, "A survey on fractional order control techniques for unmanned aerial and ground vehicles," *IEEE Access*, vol. 7, pp. 66864–66878, 2019.

[36] M. Ö. Efe, "Fractional order systems in industrial automation—A survey," *IEEE Trans. Ind. Informat.*, vol. 7, no. 4, pp. 582–591, Nov. 2011.

[37] D. Cao and J. Fei, "Adaptive fractional fuzzy sliding mode control for three-phase active power filter," *IEEE Access*, vol. 4, pp. 6645–6651, 2017.

[38] N. Liu and J. Fei, "Adaptive fractional sliding mode control of active power filter based on dual RBF neural networks," *IEEE Access*, vol. 5, pp. 27590–27598, 2017.

[39] X. Zhong, X. Shao, X. Li, Z. Ma, and G. Sun, "Fractional order adaptive sliding mode control for the deployment of space tethered system with input limitation," *IEEE Access*, vol. 6, pp. 48958–48969, 2018.
[40] N. Z. Davijani, G. Jahanfarnia, and A. E. Abharian, "Nonlinear fractional sliding mode controller based on reduced order FNPK model for output power control of nuclear research reactors," *IEEE Trans. Nucl. Sci.*, vol. 64, no. 1, pp. 713–723, Jan. 2017.
[41] S.-Y. Chen, H.-H. Chiang, T.-S. Liu, and C.-H. Chang, "Precision motion control of permanent magnet linear synchronous motors using adaptive fuzzy fractional-order sliding-mode control," *IEEE/ASME Trans. Mechatronics*, vol. 24, no. 2, pp. 741–752, Apr. 2019.
[42] G. Sun, Z. Ma, and J. Yu, "Discrete-time fractional order terminal sliding mode tracking control for linear motor," *IEEE Trans. Ind. Electron.*, vol. 65, no. 4, pp. 3386–3394, Apr. 2018.
[43] G. Sun and Z. Ma, "Practical tracking control of linear motor with adaptive fractional order terminal sliding mode control," *IEEE/ASME Trans. Mechatronics*, vol. 22, no. 6, pp. 2643–2653, Dec. 2017.
[44] S. Li, M. Zhou, and X. Yu, "Design and implementation of terminal sliding mode control method for PMSM speed regulation system," *IEEE Trans. Ind. Informat.*, vol. 9, no. 4, pp. 1879–1891, Nov. 2013.
[45] P. Pillay and R. Krishnan, "Modeling, simulation, and analysis of permanent-magnet motor drives. I. The permanent-magnet synchronous motor drive," *IEEE Trans. Ind. Appl.*, vol. 25, no. 2, pp. 265–273, Mar./Apr. 1989.
[46] G.-J. Wang, C.-T. Fong, and K. J. Chang, "Neural-network-based self-tuning PI controller for precise motion control of PMAC motors," *IEEE Trans. Ind. Electron.*, vol. 48, no. 2, pp. 408–415, Apr. 2001.
[47] S. Li, K. Zong, and H. Liu, "A composite speed controller based on a second-order model of permanent magnet synchronous motor system," *Trans. Inst. Meas. Control*, vol. 33, no. 5, pp. 522–541, 2011.
[48] X. Zhang, L. Sun, K. Zhao, and L. Sun, "Nonlinear speed control for PMSM system using sliding-mode control and disturbance compensation techniques," *IEEE Trans. Power Electron.*, vol. 28, no. 3, pp. 1358–1365, Mar. 2013.
[49] H. Liu and S. Li, "Speed control for PMSM servo system using predictive functional control and extended state observer," *IEEE Trans. Ind. Electron.*, vol. 59, no. 2, pp. 1171–1183, Feb. 2012.
[50] R. Errouissi, M. Ouhrouche, W.-H. Chen, and A. M. Trzynadlowski, "Robust nonlinear predictive controller for permanent-magnet synchronous motors with an optimized cost function," *IEEE Trans. Ind. Electron.*, vol. 59, no. 7, pp. 2849–2858, Jul. 2012.
[51] J. Zhou and Y. Wang, "Adaptive backstepping speed controller design for a permanent magnet synchronous motor," *IEE Proc.-Electr. Power Appl.*, vol. 149, no. 2, pp. 165–172, Mar. 2002.
[52] N. T.-T. Vu, H. H. Choi, and J.-W. Jung, "Certainty equivalence adaptive speed controller for permanent magnet synchronous motor," *Mechatronics*, vol. 22, no. 6, pp. 811–818, Sep. 2012.
[53] S. Li and Z. Liu, "Adaptive speed control for permanent-magnet synchronous motor system with variations of load inertia," *IEEE Trans. Ind. Electron.*, vol. 56, no. 8, pp. 3050–3059, Aug. 2009.
[54] H. H. Choi, N. T.-T. Vu, and J.-W. Jung, "Digital implementation of an adaptive speed regulator for a PMSM," *IEEE Trans. Power Electron.*, vol. 26, no. 1, pp. 3–8, Jan. 2011.
[55] T.-L. Hsien, Y.-Y. Sun, and M.-C. Tsai, "H^{∞} control for a sensorless permanent-magnet synchronous drive," *IEE Proc.-Electr. Power Appl.*, vol. 144, no. 3, pp. 173–181, May 1997.
[56] Y. X. Su, C. H. Zheng, and B. Y. Duan, "Automatic disturbances rejection controller for precise motion control of permanent-magnet synchronous motors," *IEEE Trans. Ind. Electron.*, vol. 52, no. 3, pp. 814–823, Jun. 2005.
[57] H. H. Choi and J. W. Jung, "Discrete-time fuzzy speed regulator design for PM synchronous motor," *IEEE Trans. Ind. Electron.*, vol. 60, no. 2, pp. 600–607, Feb. 2013.
[58] F. F. M. El-Sousy, "Robust wavelet-neural-network sliding-mode control system for permanent magnet synchronous motor drive," *IET Electr. Power Appl.*, vol. 5, no. 1, pp. 113–132, 2011.
[59] F. M. Zaihidee, S. Mekhilef, and M. Mubin, "Robust speed control of PMSM using sliding mode control (SMC)—A review," *Energies*, vol. 12, no. 9, p. 1669, 2019.
[60] Y. Chen, I. Petras, and D. Xue, "Fractional order control—A tutorial," in *Proc. ACC*, St. Louis, MO, USA, Jun. 2009, pp. 1397–1411.
[61] I. Podlubny, *Fractional Differential Equations*. New York, NY, USA: Academic, 1999.
[62] K. B. Oldham and J. Spanier, *The Fractional Calculus*. New York, NY, USA: Academic, 1974.
[63] I. Podlubny, "Geometric and physical interpretation of fractional integration and fractional differentiation," *Fract. Calc. Appl. Anal.*, vol. 5, no. 4, pp. 367–386, 2002.
[64] D. Matignon, "Stability results for fractional differential equations with applications to control processing," *Comput. Eng. Syst. Appl.*, vol. 2, pp. 963–968, Jul. 1996.

FARDILA M. ZAIHIDEE received the B.Eng. degree in electrical engineering from the Hochschule der Technik und Wirtschaft des Saarlandes, Saarbruecken, Germany, in 2006, and the M.Eng. degree in mechatronics from the University of Malaya, Kuala Lumpur, Malaysia, in 2013.

She is currently pursuing the Ph.D. degree in electrical engineering with the University of Malaya, Kuala Lumpur. She is also a Lecturer with the Engineering Technology Department, Sultan Idris Educational University. Her research interests include motor drives and automation and control.

SAAD MEKHILEF is currently a Professor with the Department of Electrical Engineering, University of Malaya. He is also the Director of the Power Electronics and Renewable Energy Research Laboratory—PEARL. He has authored or coauthored of more than 250 publications in international journals and proceedings. He is actively involved in industrial consultancy for major corporations in the power electronics projects. His research interests include power conversion techniques, control of power converters, renewable energy, and energy efficiency. He is a Fellow of IET. He is an Associate Editor of the IEEE TRANSACTIONS ON POWER ELECTRONICS and *Journal of Power Electronics*.

MARIZAN MUBIN was born in Kuala Lumpur, Malaysia, in 1977. She received the B.Eng. degree in telecommunication engineering from the University of Malaya, Kuala Lumpur, in 2000, the M.Sc. degree in communications and signal processing from the University of Newcastle Upon Tyne, U.K., in 2001, and the D.Eng. degree in electrical engineering from Tokai University, Japan, in 2006.

She is currently a Senior Lecturer with the Department of Electrical Engineering, University of Malaya, Kuala Lumpur.